Pure Appl. Chem., Vol. 76, Nos. 7–8, pp. 1547–1561, 2004.

Engineering DNA aptamers and DNA enzymes with fluorescence-signaling properties*

Razvan Nutiu†, Shirley Mei†, Zhongjie Liu†, and Yingfu Li‡

Department of Biochemistry and Department of Chemistry, McMaster University, Hamilton, Ontario L8N 3Z5, Canada

Abstract: Single-stranded DNA molecules with ligand-binding ability and catalytic function, referred to as DNA aptamers and DNA enzymes, respectively, are special DNA sequences isolated from random-sequence DNA libraries by "in vitro selection". These two new classes of artificial DNA molecules have the potential of being used as molecular tools in a variety of innovative applications ranging from biosensing to gene regulation. Our laboratory is interested in engineering fluorescence-signaling DNA aptamers and DNA enzymes that can be widely exploited for detection-directed applications. In this article, we will first discuss our recent efforts on the rational design of a new class of signaling aptamers denoted "structure-switching signaling aptamers", which report target binding by switching structures from DNA/DNA duplex to DNA/target complex. We will then describe the in vitro selection of fluorescence-signaling DNA enzymes that exhibit a synchronized catalysis-signaling capability by cleaving a chimeric RNA/DNA substrate at the lone RNA linkage surrounded by a closely spaced fluorophore-quencher pair. Potential utilities of these signaling DNA molecules will also be discussed.

INTRODUCTION

Nucleic acids have been traditionally exploited as affinity probes for the detection of DNA and RNA targets based on their abilities to form DNA/DNA or DNA/RNA duplexes. Several landmark discoveries over the past two decades—including the revelation of natural RNA enzymes (ribozymes) and the demonstration that DNA or RNA molecules with novel catalytic or binding capabilities can be created in vitro [1–6]—have significantly broadened the utility of nucleic acids as molecular recognition elements. DNA and RNA can now be engineered not only to detect nucleic acid targets, but also to recognize a broad scope of non-nucleic acid ligands including proteins and metabolites [7,8].

Aptamers are single-stranded DNA or RNA molecules isolated from large pools of random-sequence oligonucleotides to bind a wide range of chemical or biological entities with high affinity and specificity [5–8]. Similar to antibodies, aptamers can be used as molecular recognition elements in analytical detection systems. DNA aptamers offer several advantages over their protein-made analogs. The isolation of aptamers is done in vitro, and the target for aptamer creation can be any molecule, including toxins. Once a DNA aptamer is identified, it can be reproduced by automated DNA synthesis at very low cost and with a high batch-consistence. Moreover, DNA aptamers are easy to modify to introduce various reactive groups, affinity tags, or reporting moieties that may be needed for a particular application. Finally, DNA aptamers have a long shelf-life and usually stay active following a denaturation–renaturation process.

---

*Lecture presented at the symposium "Chemistry of nucleic acids", as part of the 39th IUPAC Congress and 86th Conference of the Canadian Society for Chemistry: Chemistry at the Interfaces, Ottawa, Canada, 10–15 August 2003. Other Congress presentations are published in this issue, pp. 1295–1603.

†These three authors have made equal contributions to this work.

‡Corresponding author: Tel: (905) 525 9140 ext. 22462; Fax: (905) 522 9033; E-mail: liying@mcmaster.ca

DNA enzymes, also known as deoxyribozymes or DNAzymes, refer to single-stranded DNA molecules with catalytic capabilities. Similar to DNA aptamers, DNA enzymes are generated de novo by in vitro selection from an extraordinarily large population of single-stranded DNA molecules. Since the report of the first DNAzyme nearly 10 years ago [4], hundreds of DNA sequences have been isolated in many research laboratories around the world to facilitate more than a dozen chemical transformations of biological relevance [9–12]. For example, DNA enzymes have been isolated to cleave DNA [13] and RNA [4,14], ligate RNA [15], and phosphorylate DNA [16]. In recent years, considerable efforts have been undertaken to develop DNA enzymes as reporter molecules for biosensing applications or as agents to regulate gene expression at RNA level [12].

One important step in developing a biosensing system that exploits DNA aptamers and DNA enzymes is to establish effective methods capable of transducing a binding and/or catalytic event into an easily recordable signal. Strategies have been devised for transducing aptamer–target interactions into electrochemical, mechanical, piezoelectric, or fluorescent signals [17–20]. Within these methods, fluorescence signaling is very desirable because of the convenience of detection, the diversity of measurement methods, and the availability of a large selection of fluorophores and quenchers for nucleic acid modification [21]. Therefore, exploring various strategies for the design of effective fluorescence-signaling aptamers is a research subject actively pursued by several research groups [22–29]. Similarly, fluorescence-based sensor molecules made of DNA enzymes have also been reported in a number of studies [30–35]. In this article, we will discuss some recent results from our group in the pursuit of new ways to create signaling DNA aptamers or signaling DNA enzymes [29,34,35] by rational design or by in vitro selection and evolution.

RESULTS AND DISCUSSION

Rational design of structure-switching signaling DNA aptamers

Standard DNA aptamers do not possess intrinsic fluorescence-signaling capabilities when they are isolated from random-sequence libraries and can only be made fluorescent through postselection modifications by rational design. A desirable rational design strategy should be one that can be easily applied to any given aptamer regardless of its size and structural properties. This is important because aptamers are known to have variable sizes and vastly different secondary and tertiary structures. Some aptamers do not have an easily determinable secondary structure, and the tertiary structures of most aptamers are not readily available. Equally important is the effectiveness of the design method in generating signaling aptamers with a large signaling magnitude, a fast response time or a real-time signaling capability. Signaling aptamers exhibiting large fluorescence enhancements upon target binding increase the sensitivity and accuracy of signaling aptamer-based assays. The real-time reporting capability should allow rapid sample measurements and permit the integration of signaling aptamers into demanding applications such as high-throughput screening.

We have conceived a rational design strategy based on the universal capability of DNA aptamers to adopt two different forms of structures: a duplex structure with a complementary DNA sequence and a complex structure with the target for which the aptamer is created. In the particular design illustrated in Fig. 1A, three DNA oligonucleotides are used: FDNA, QDNA, and MAP. MAP stands for a modified aptamer sequence containing a target-binding element (in black) and non-target-binding motif (in gray). MAP is designed to possess the capability to form two short duplexes with FDNA (labeled with a fluorophore) and QDNA (labeled with a fluorescence quencher), respectively. In this arrangement, the fluorophore and the quencher are located in close proximity and a low level of fluorescence ensues. The introduction of the target promotes the aptamer to adopt a more stable complex structure. In this new structural configuration, only FDNA is able to bind the MAP-target complex. The departure of QDNA from the original duplex assembly results in the separation of the quencher from the fluorophore and, therefore, an increase of fluorescence intensity. A rapid transition from the duplex state to the complex

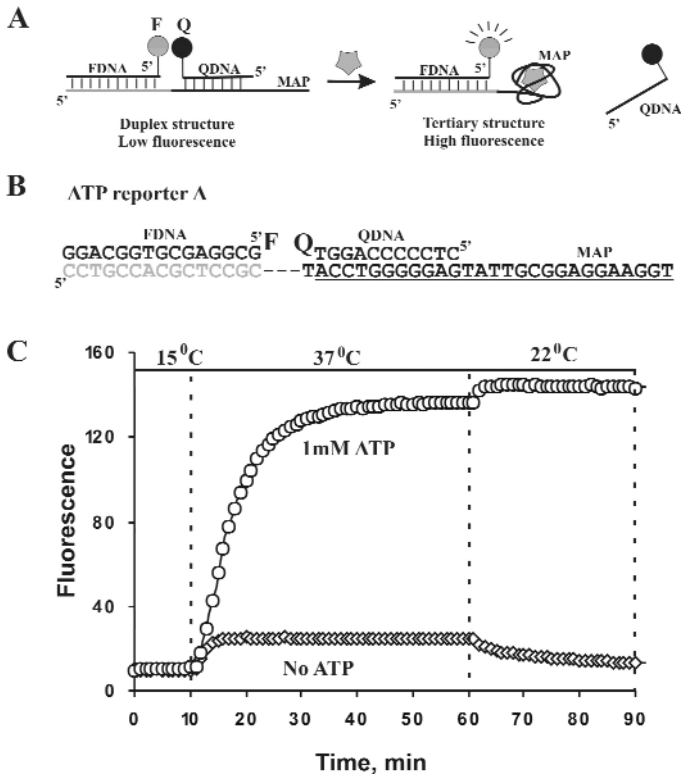

Fig. 1 Design of structure-switching signaling aptamers. (A) Working principle. A tripartite, fluorescence-quenching, two-stem duplex assembly can be constructed using a fluorophore (*F*)-containing FDNA, a quencher (*Q*)-containing QDNA, and an unmodified DNA molecule (MAP) that contains an FDNA-binding sequence (in gray) and a target-binding motif (in black). When the target (gray star) is introduced, the duplex structure is transformed into the target-aptamer complex with a concomitant release of QDNA and an enhancement of fluorescence intensity. **(B)** An ATP-binding aptamer as a model system. The original 27-nt aptamer (underlined) is appended with a sequence at the 5′-end for the formation of the 15-bp duplex with FDNA. An 11-nt QDNA containing a DABCYL at the 3′-end is used as a quencher. **(C)** Evidence for structure switching from a temperature-changing experiment. Data points in diamonds are for samples containing no ATP and those in circles for ATP-containing solutions. Temperature settings are indicated on the top of the graph. The fluorescence intensity was measured every minute when the temperature of each solution was changed as follows: a 10-min incubation at 15 °C, followed by a temperature increase to 37 °C within 1 min and further incubation at this temperature for 50 min. Finally, each sample was cooled to 22 °C in 1 min and incubated at 22 °C for 30 more minutes.

state promoted by target addition would offer a general reporting system capable of monitoring the binding process in real time.

A previously isolated ATP aptamer [36] that is known to bind two ATP molecules in its structure fold [37] has been used as a model aptamer for the proof of the above concept (Fig. 1B).

The length of QDNA is an important factor for consideration. It should have an adequate size so that it anneals to MAP with moderate strength to offer both low background fluorescence in the absence of the target and a possibility for fast structure switching when the target is present. Consequently, we tested a series of QDNAs with different number of nucleotides (data not shown) and chose an 11-nt sequence that showed both a low melting point (desirable for target-induced structure switch) and a low level of background fluorescence (indicative of a stable QDNA/MAP duplex).

The behavior of the above anti-ATP signaling aptamer system (denoted ATP Reporter A) in the presence and absence of ATP was studied under different temperature settings. The evidence of struc-

ture-switching was obtained using the simple temperature-changing experiment shown in Fig. 1C. We incubated both 1 mM ATP-containing (data series shown in circles) and ATP-lacking (diamonds) signaling aptamer solutions for a total of 90 min at different temperature settings—the first 10 min at 15 °C, the next 50 min at 37 °C, and the final 30 min at 22 °C. Rapid structure-switching was not observed at 15 °C (indicated by steady fluorescence observed for both solutions) because the preformed FDNA/QDNA/MAP duplex assembly was too stable at this temperature and ATP was not able to displace QDNA. Structure transition occurred at 37 °C (indicated by the progressive fluorescence intensity increase in the ATP-containing sample) because the duplex assembly was weakened at this temperature, allowing ATP to gradually replace QDNA molecules in the assembly. When the temperature was dropped to 22 °C, while free QDNA molecules reassembled back onto MAP in the ATP-lacking solution, the formation of the ATP-aptamer complex in the ATP-containing solution prevented the QDNA from re-annealing to MAP.

The ATP reporter described above exhibited fairly slow target-induced fluorescence intensity increase at low temperature range (at 15 °C or room temperature, data not shown). This slow response can be attributed to the relative high stability of the MAP/QDNA duplex. Since weakening the duplex by simply shortening the size of QDNA would significantly increase the level of background fluorescence, the exploration of alternative arrangements became a necessity. One successful strategy we devised was to insert a "nonsense" sequence of five nucleotides between the aptamer domain and the FDNA binding domain in MAP (Fig. 2A, the portion of the sequence written in italicized letters). A 12-nt QDNA was then designed to bind these five nucleotides, as well as the seven adjacent nucleotides on the aptamer element. We hypothesized that it should be easier for ATP to compete with fewer nucleotides that block the target-binding site in the aptamer (7 nt in the new design vs. 11 nt in the old design) while overall stability of QDNA/MAP duplex would be maintained. After the formation of ATP-aptamer complex, the remaining duplex between QDNA and five nucleotides in MAP would not be strong enough to hold QDNA onto MAP. Indeed, when the newly designed reporter (denoted ATP Reporter E) was exposed to the target, the structure-switching process took place in less then 2 min in a temperature-independent manner (Fig. 2B) and a more than 10-fold fluorescence enhancement was observed. ATP reporter E was sensitive to the change of target concentration and exhibited a linear response when ATP concentration was varied between 0.01 and 1 mM (Fig. 2C). ATP reporter E can also discriminate, to a certain extent, compounds with a high degree of structural similarity including adenosine, AMP, ADP, ATP, and dATP. As expected, it did not respond to the addition of other nonanalogous nucleotides such as GTP, CTP, and UTP (Fig. 2D) as it had been previously shown that the original DNA aptamer has no affinity for these nucleotides [36].

To confirm that the above-described design strategy is generally applicable, we successfully designed one more structure-switching signaling aptamer (Fig. 3A) using another previously isolated DNA aptamer, which interacts with a protein target, thrombin, and has a completely different tertiary structure, size, and affinity for its target [38,39]. The thrombin reporter displayed characteristics similar to ATP reporter E: it generated a fast signal response to the addition of thrombin at 25 °C and above (Fig. 3B), it showed a linear response when the thrombin concentration was changed between 0.05–1 μM (Fig. 3C) and it discriminated between different forms of thrombins (α, β, and γ thrombins) and other related or unrelated proteins such as human factors IXa, Xa, and BSA (Fig. 3D). The thrombin reporter was less effective than the ATP reporter E with regard to the speed of real-time response to the target addition at room temperature. This can be justified by the size difference between the two aptamers. The anti-thrombin aptamer (15 nt) is significantly shorter than the anti-ATP aptamer (27 nt); therefore, a 12-nt QDNA blocks 40 % nucleotides in the anti-thrombin aptamer but ony occupies 26 % nucleotides in the anti-ATP aptamer. Nevertheless, this reporter was still sufficiently responsive in real-time signaling as judged by the rapid fluorescence increase at 30 °C when 1 μM α-thrombin was used as the target.

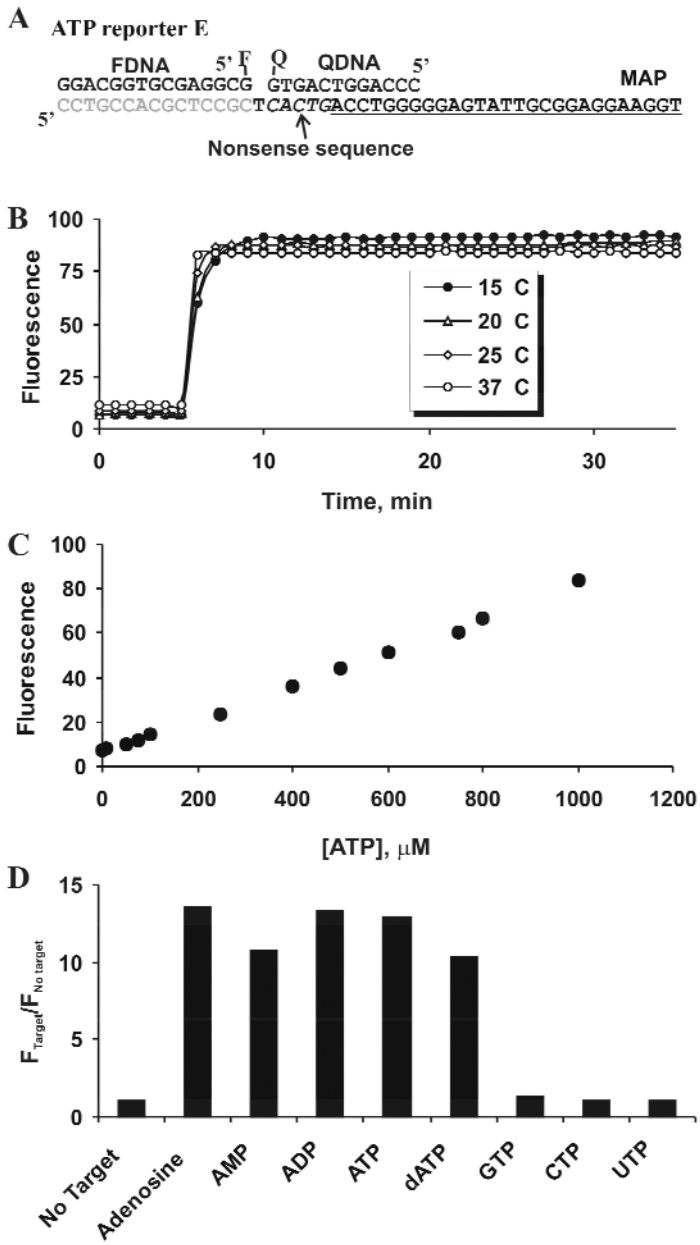

Fig. 2 An ATP reporter with real-time sensing capability at low temperature. **(A)** The DNA sequences used for the construction of ATP Reporter E. The modified aptamer contained the FDNA-binding domain (in gray), the original aptamer sequence (underlined), and an inserted 5-nt domain (italicized) as part of the QDNA-binding domain. **(B)** Real-time sensing results. ATP reporter E was incubated in the absence of ATP for 10 min at an indicated temperature (15, 20, 25, or 37 °C), followed by the addition of ATP to 1 mM and a further incubation at the same temperature for 30 more minutes. **(C)** The fluorescence intensity of ATP Reporter E in response to the change of ATP concentration. ATP concentrations were tested at 0, 10, 25, 50, 75, 100, 250, 400, 500, 600, 750, 800, and 1000 μM. Each data point represents the average value of three independent experiments. **(D)** Signaling specificity of ATP Reporter E. The fluorescence intensity of the signaling aptamer was measured in the presence of each of indicated compounds (all at 1 mM). The data are normalized as $F_{\text{Target}}/F_{\text{No target}}$, where F_{Target} is the fluorescence intensity of each sample and $F_{\text{No target}}$ is the reading for the reporter in the absence of any target.

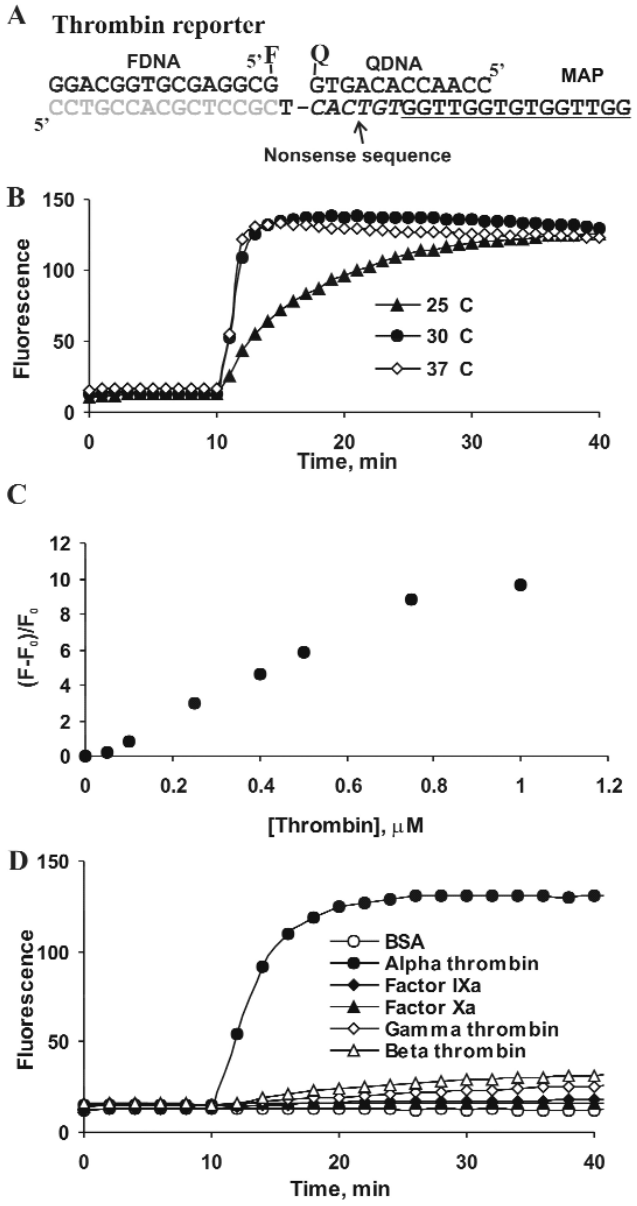

Fig. 3 A structure-switching reporter for thrombin. **(A)** Sequences of DNA molecules used. A previously isolated DNA aptamer for thrombin binding was configured into the tripartite signaling system using the similar design strategy employed for ATP reporter E (see Fig. 2A; the original thrombin-binding aptamer sequence is underlined). **(B)** Real-time sensing capability of the thrombin reporter. The reporter was examined in a similar way to that shown in Fig. 2B except that thrombin (1 μM) was used as the target. **(C)** Fluorescence response of the reporter to thrombin concentration, which was used at 0, 10, 50, 100, 250, 400, 500, 750, and 1000 nM. The fluorescence intensity of the thrombin reporter was recorded in real time at 30 °C with different concentrations of thrombin (in triplicate) using the same experimental setting as in Fig. 2B. The fluorescence intensity at the 20th minute for each sample is normalized as $(F - F_0)/F_0$, where F is the fluorescence intensity of each sample; F_0 is for the sample containing no thrombin. Each data point represents the average value of three independent experiments. **(D)** Signaling specificity of the thrombin reporter. Real-time assay was conducted in the absence of any protein ligand (data not shown) and in the presence of BSA, factor Xa, factor IXa, and human thrombin α, β, and γ, respectively. Each protein was used at 0.75 μM.

It is worth commenting on the affinity alteration by QDNA to the original aptamers. The use of QDNA reduced the affinity of the ATP aptamer by 60-fold (K_d was changed from ~10 μM in the original aptamer to ~600 μM in the modified aptamer) while only lessened the affinity of the thrombin aptamer by 2-fold (from ~200 to ~400 nM). This observation seems to suggest that the structure-switching-based modification strategy may cause more affinity reduction to low-affinity aptamers than to high-affinity ones. Although certain degree of affinity reduction to an aptamer may not significantly diminish the utility of the aptamer reporter, it is certainly preferred that the affinity reduction be kept at minimum. Since all QDNAs tested so far are DNA molecules that are completely complementary to the modified aptamers, it is conceivable that one potential way to minimize the affinity decrease is to use QDNAs with sequences that form less perfect duplexes with the aptamer. This and other strategies will be investigated in the future.

In vitro selection of efficient signaling DNA enzymes

Another major interest in our laboratory is to develop a fluorescence-signaling biosensor system based on the catalytic capability of DNA. Although sensor molecules made of DNA enzymes have been reported by several groups [30–33] prior to our studies, they were constructed using existing DNA enzymes that were not created specifically for signaling applications and are less optimal in their signaling properties. Therefore, our goal was to make special DNA enzymes that can couple fluorescence signaling with efficient catalysis.

First, we designed a special DNA/RNA chimeric substrate (denoted A1 in Fig. 4) containing a single ribonucleotide as the cleavage site (Ar, Fig. 4B) as well as a fluorophore (*F*) and a quencher (*Q*) covalently linked to the deoxyribonucleotides that sandwich the RNA site. This substrate has a very low level of background fluorescence, but it can generate a large fluorescence signal upon the cleavage of the RNA linkage. Next, we sought DNA enzymes that could efficiently cleave this specially arranged RNA junction by in vitro selection. We employed the in vitro selection scheme shown in Fig. 4A to isolate signaling DNA enzymes based on their ability to perform catalysis in a *cis*-acting manner, meaning that the substrate is covalently attached to the DNAzyme. The selection scheme contains eight steps. In step I, a pool of single-stranded 86-nt DNA containing 43 random-sequence nucleotides was first ligated to the substrate DNA A1 (23-nt) containing the three key moieties described above (all DNA sequences are given in Fig. 4B). The ligated 109-nt DNA was purified by PAGE in step II, followed by step III where the modified DNA molecules were incubated in the reaction mixture (containing 400 mM NaCl, 100 mM KCl, 7.5 mM $MgCl_2$, 5 mM $MnCl_2$, 1 mM $CoCl_2$, 0.25 mM $NiCl_2$, and 1.25 mM $CdCl_2$ in 50 mM HEPES, pH 6.8 at 23 °C). Any autocatalytic DNA capable of cleaving the lone RNA linkage was expected to produce a 94-nt DNA fragment that could be isolated by PAGE in step IV. The recovered DNA was amplified by two successive polymerase chain reactions (PCRs). The first PCR was carried out with the use of primers P1 and P2 (step V). The second PCR (step VI) used P1 and P3. Since P3 was a ribo-terminated primer, the double-stranded DNA product generated in the second PCR step contained a single ribonucleotide linkage. The DNA product from the second PCR was treated with NaOH (step VII) under conditions that could fully cleave the ribonucleotide linkage (0.25 M NaOH, 90 °C, 10 min). The digested DNA mixture was subjected to PAGE purification. The sense strand was recovered and phosphorylated (step VIII). The resulted 5′-phosphorylated DNA was used to initiate the next round of selection.

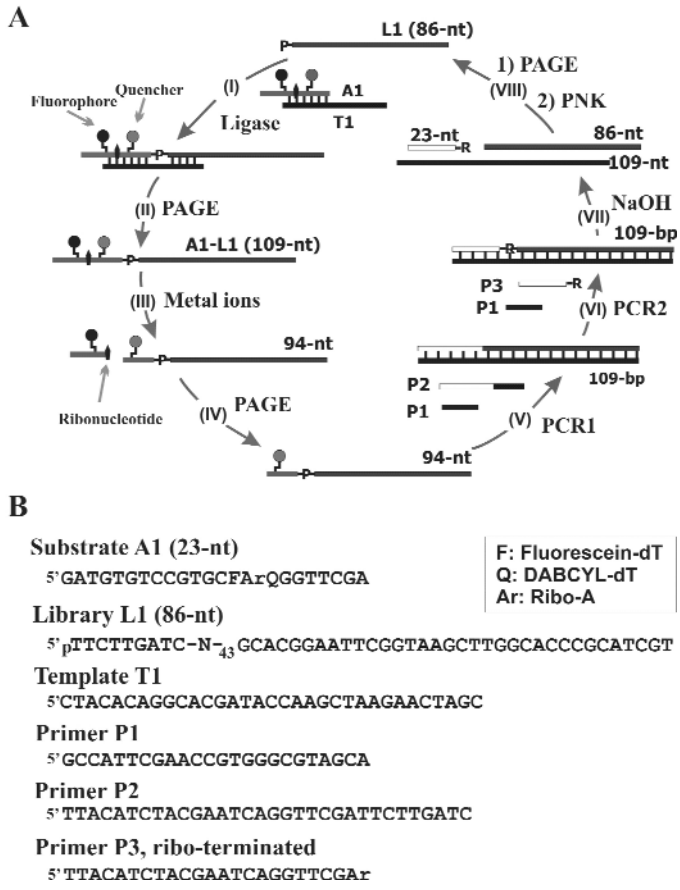

Fig. 4 In vitro selection of signaling DNA enzymes. (A) Selection scheme. Each selection cycle consists of steps I–VIII as described in main text. (B) Sequences of the DNA pool (L1), substrate A1, and template T1, and the primers for PCR. N_{43} is the random domain.

Beginning with a population of 10^{14} different DNA molecules we successfully isolated, after 22 rounds of selection, a DNA enzyme that is capable of coupling RNA cleavage with fluorescence signaling. This catalytic DNA was named DEC22-18, and its sequence is given in Fig. 5A. Following in vitro selection, we assessed DEC22-18 for divalent metal ion dependence and found that the catalytic function of this DNA enzyme needs the support of some of the divalent metal ions (namely Co^{2+}, Ni^{2+}, or Mn^{2+}) that were included in the original selection mixture. Further investigation revealed that Co^{2+} was the preferred divalent metal ion. The elimination of monovalent metal ions Na^+ and K^+ slightly enhanced the enzymatic activity of DEC22-18. Based on these observations, we conducted a series of experiments to derive the most optimal salt and pH conditions for DEC22-18. This effort led to the finding that this DNA enzyme was most effective in 10 mM of Co^{2+}, 5 mM Mg^{2+}, and 50 mM HEPES at pH 6.8.

The original DEC22-18 contained 109 nt (including the substrate A1 domain). Deletion experiments using synthetic DNAs led to a shortened version of DNA enzyme (83 nt) named DEC22-18A (Fig. 5B). Under aforementioned optimal reaction conditions, the cleavage reaction of DEC22-18A proceeded too fast to allow an accurate measurement of rate constant by manual quenching method. Based on the observation that nearly 50 % of DEC22-18A self-cleaved in 3 s, we estimated that the *cis*-acting DEC22-18A possesses a k_{obs} of more than 10 min^{-1}. We also determined the rate constant of the un-

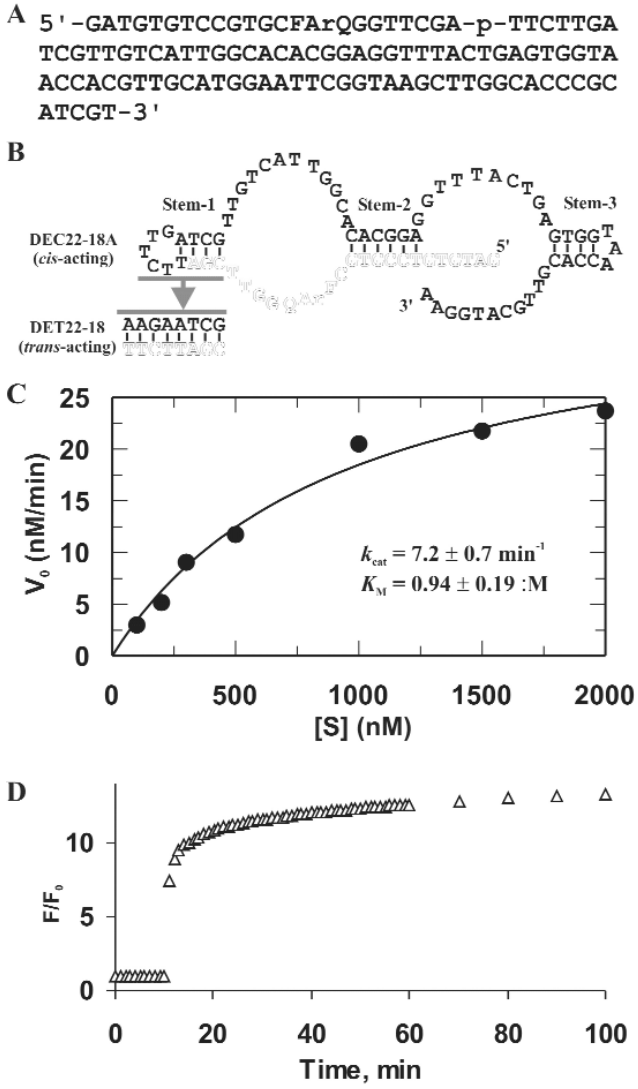

Fig. 5 DEC22-18—an efficient RNA-cleaving DNA enzyme with fluorescence-signaling capability. (A) Sequence of DEC22-18. Ar: adenosine ribonucleotide; F: fluorescein-dT; Q: DABCYL-dT. (B) Putative secondary structure of DEC22-18A (a shortened version of DEC22-18) predicted by *mfold* program. The sequence of a *trans*-acting enzyme, DET22-18 is shown in solid letters and that of the substrate (denoted S1) is shown in hollow letters. (C) Kinetic analysis of DET22-18. Substrate S1 was labeled at the 5′-end with [γ-^{32}P]ATP and PNK. 5 nM of DET22-18 was incubated with substrate concentrations at 100, 200, 300, 500, 1000, 1500, and 2000 nM in a reaction buffer containing 10 mM $CoCl_2$ and 5 mM $MgCl_2$ in 50 mM HEPES (pH 6.8, 23 °C). The velocity at different substrate concentrations were fit to the Michaelis–Menten equation using the GraFit software. Experiments were conducted in triplicate, and the average velocity at each substrate concentration is shown in graph. (D) Real-time signaling profile of DET22-18/S1 system. S1 was incubated at room temperature in the absence of DET22-18 for 10 min, followed by the addition of DET22-18 and a further incubation at the same temperature for an additional 90 min. The fluorescence intensity was recorded every minute for the first 60 min and every 10 min thereafter. The DNA concentrations were as follows: S1 at 0.5 μM, DET22-18 at 5 μM. The reaction mixture also contained 50 mM HEPES, pH 6.8 (determined at 23 °C), 14 mM $MgCl_2$, and 1 mM $CoCl_2$. F_0 is the initial fluorescence, and F is the intensity at a given time point.

catalyzed cleavage reaction under the same reaction conditions, which was 6×10^{-7} min^{-1}. Therefore, we can conclude that DEC22-18A affords a rate enhancement in the neighborhood of 17 million-fold under the optimized conditions.

A secondary structure for DEC22-18A (Fig. 5B) was predicted using *mfold* computer folding program [40]. Based on this secondary structure, we engineered a true enzyme that is able to perform cleavage in an intermolecular fashion (Fig. 5B). The *trans*-acting DNA enzyme was named DET22-18. We further found that the cleavage reaction by DET22-18 followed Michaelis-Menten kinetics. The catalytic rate constant, k_{cat}, and the Michaelis constant, K_M, were determined under multiple-turnover conditions (Fig. 5C) in which an excess substrate (from 0 to 2000 nM) was used against a fixed concentration of enzyme (5 nM). A k_{cat} of 7.2 ± 0.7 min^{-1} and a K_M of 0.94 ± 0.19 μM were calculated, leading to the conclusion that DET22-18 is the second fastest DNA enzyme reported to date, with a speed closely matching the k_{cat} value reported for the "10-23" DNA enzyme derived by Santoro and Joyce [14].

As we anticipated, both *cis*- and *trans*-versions of the DNA enzyme can generate fluorescence as a result of chemical action. Figure 5D shows a fluorescence assay under the enzyme: substrate ratio of 10:1. The system had a steady fluorescence (first 10 min of the reaction) when S1 (substrate) was incubated with 1 mM Co^{2+} without DET22-18. When the DNA enzyme was added, the fluorescence intensity of the reaction mixture increased sharply. The fluorescence enhancement increased at such a rapid rate that within 1 min, 7.4-fold enhancement was observed. Similar signaling profile was also obtained when enzyme-to-substrate ratio was set at 1:10, consistent with the multiple-turnover capability of DET22-18.

Finally, we wanted to prove our conceptual biosensor system using DEC22-18, along with the use of an existing DNA aptamer. By adjoining the DNAzyme with an aptamer, we aimed to rationally engineer our DNA enzyme into a catalytic system that could be allosterically regulated by a small molecule. Using the rational design strategy developed for the engineering of many allosteric ribozymes [41–50], we attempted to adjoin DEC22-18A with the previously derived anti-ATP DNA aptamer [36] that was also used for the structure-switching signaling aptamer project described above. The fundamental principle behind allosteric nucleic acid enzyme engineering was to link a catalytic domain (a DNA enzyme or ribozyme) to a binding element (a DNA or RNA aptamer) through a so-called "communication module" [41] that can translate the target binding to enzyme action. In our particular design, the anti-ATP DNA aptamer was linked to the catalytic domain of DEC22-18 through a very weak stem (labeled as stem-1; Fig. 6A). A high level of catalysis by such an arranged catalytic domain would occur only if stem-1 is able to form. However, the formation of stem-1 is dependent on ATP-promoted tight structure folding of the aptamer domain. Without ATP, the aptamer domain could not fold tightly to strengthen the weakened stem-1; consequently, catalysis could only proceed slowly (see Fig. 6B for a graphic explanation in which ATP is the intended target and GTP is used as a control for which the anti-ATP aptamer has no affinity). We found that the allosteric DNA enzyme design shown in Fig. 6A was indeed able to perform real-time detection of ATP (Fig. 6C; triangles: ATP as target; squares: GTP as a control; each target was added to the allosteric DNA enzyme reaction solution following a 10-min incubation in the absence of any target). This enzymatic reporter displayed a nearly 20-fold rate enhancement in the presence of ATP over GTP. The success in constructing this prototype allosteric deoxyribozyme serves as a positive step in our continuing pursuit of a robust sensor system exploiting the catalytic capability of DNA.

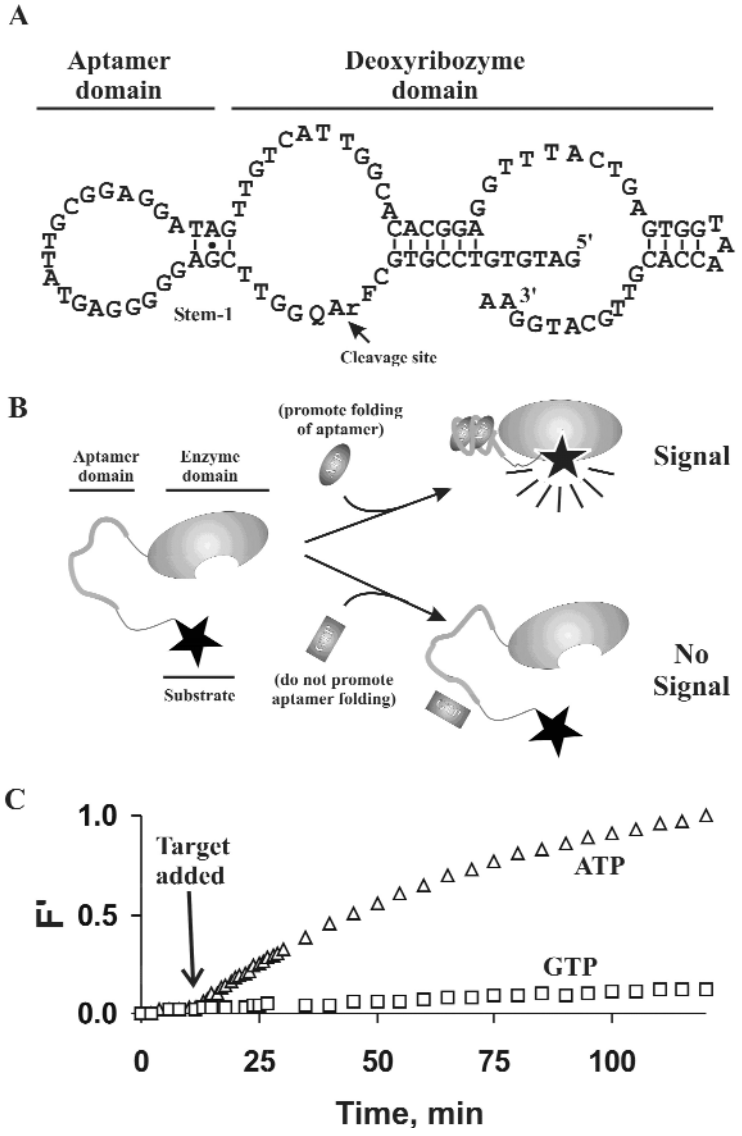

Fig. 6 An ATP-dependent allosteric DNA enzyme. (A) DEC22-18A is conjugated with a known anti-ATP DNA aptamer through a weakened stem-1 as a communication module. (B) A schematic representation of the action by the designed allosteric DNA enzyme. The aptamer domain (shown as thick gray line) that can bind specifically to ATP is covalently linked to the DNA enzyme domain and the substrate. Binding of two ATP molecules to the aptamer domain induces a conformational change that leads to the stabilization of stem 1 and the activation of catalysis. (C) Activation by ATP vs. GTP. The DNA molecule was incubated at 37 °C in the absence of ATP and GTP for 10 min, followed by the addition of 1 mM ATP (triangle) or GTP (square) and incubated for an additional 110 min at the same temperature. The fluorescence intensity was recorded every minute for the first 30 min and then every 5 min thereafter. The reaction mixture contained 40 nM DNA along with 0.25 mM $CoCl_2$, 14 mM $MgCl_2$, 400 mM NaCl, 100 mM KCl, 50 mM HEPES (pH 6.8 measured at 23 °C). The fluorescence intensity was normalized as $F' = (F - F_0)/(F_{max} - F_0)$ where F is the fluorescence reading of a solution at any given time point, F_0 is the reading of each sample made at the starting point, and F_{max} is the reading made at 120 min for the ATP-containing sample.

In vitro selection of signaling DNA enzymes with various pH optima

Encouraged by our success in the creation of an efficient DNA enzyme with a synchronized catalysis and fluorescence-signaling capability and by the potential utility of such enzymatic molecules in biosensing applications, we conducted another in vitro selection study aimed to create more DNA enzymes with similar signaling capabilities but with broad pH dependences. The first goal of the study was to create fluorescence-signaling deoxyribozymes with different pH profiles to allow for biosensing applications to be conducted effectively under different solution conditions. The second goal was to determine whether DNA has the ability to perform catalysis under very demanding reaction conditions such as an extremely high acidity (pH 3 and 4).

Substrate A1 used in the previous study (with a ribonucleotide as the cleavage site, which is sandwiched by a pair of fluorophore and quencher) was adopted for this new effort once again. Therefore, the new DNA enzymes to be derived would perform the same RNA cleavage reaction and should possess similar fluorescence-signaling capabilities. A new population of 10^{14} different DNA molecules of 100 nucleotides in length (70 of which were random nucleotides, vs. 43 in the previous study) was synthesized. Using a similar selection strategy as before, we carried out seven repetitive rounds of selection and amplification at pH 4.0 to establish a catalytic DNA pool. Starting with this derived pool, diverse DNA enzymes were evolved through five parallel paths of in vitro evolution under pH 3.0, 4.0, 5.0, 6.0, and 7.0, respectively. After many more rounds of mutagenesis, selection and amplification for each path, five new catalytic populations were derived that exhibited efficient catalysis under each given pH condition. The sequences of the most dominant catalyst from each path (named pH3DZ1, pH4DZ1, pH5DZ1, pH6DZ1, and pH7DZ1) are shown in Fig. 7A. The details of the in vitro selection and in vitro evolution experiment have been published elsewhere [35].

The pH dependence of the catalytic activity was determined for these five deoxyribozymes (Fig. 7B). We found that the DNA enzymes selected at pH 3–6 showed the maximum catalytic rate constants at or near the pH at which they were selected. Each DNA enzyme exhibited a relatively narrow pH range within 3 pH units. The only catalytic DNA that did not show a pH maximum is pH7DZ1, whose catalytic rate constant rose with an increased pH from 5.5 to 8.0. These findings indicate that the pH dependence of the final DNA enzymes was largely controlled by the pH setting used during the selection step. Most of the DNA enzymes (namely, pH4DZ1, pH5DZ1, pH6DZ1, and pH7DZ1) showed fairly large catalytic rate constants (k_{obs} in the range of 0.2 to 1.3 min^{-1}). However, pH3DZ1 was 10 times less efficient, with a k_{obs} of 0.023 min^{-1}. These DNA enzymes have also been assessed for the fluorescence-generating capability upon catalysis and were found to possess expected signaling behaviors with variable signaling magnitude (data not shown), suggesting that they could be exploited as catalytic reporters.

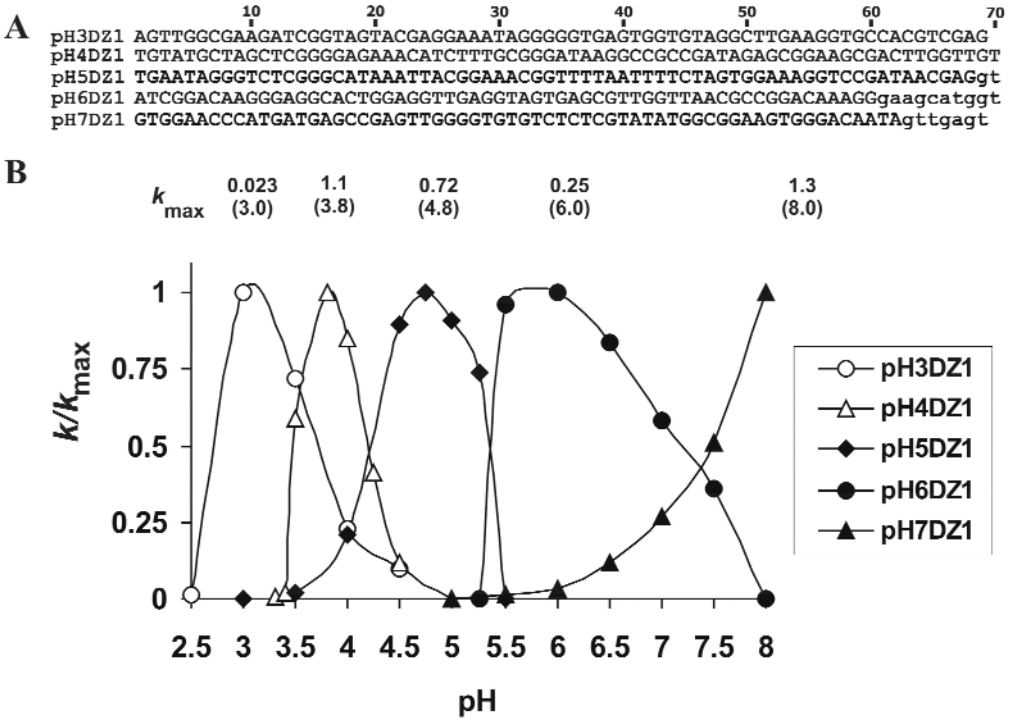

Fig. 7 Signaling DNA enzymes with various pH profiles. (A) Sequences of the dominant deoxyribozymes. Each catalyst also contains GATGT GTCC GTGCF RQGGT TCGAG GAAGA GATGG CGAC (F: fluorescein-dT; R: ribo-A; Q: DABCYL-dT) at the 5′-end and AGCTG ATCCT GATGG at the 3′-end. Nucleotides shown in small letters (as well as nucleotides after them) in pH5DZ1, pH6DZ1, and pH7DZ1 are not required for catalysis. The last 15 nucleotides in the 3′ end of pH3DZ1 are not needed for catalytic activity while the first 6 nucleotides (AGCTGA) in the same region are required by pH4DZ1. (B) Normalized catalytic rates vs. pH for the 5 dominant deoxyribozymes. k is the rate constant at a given pH, and k_{max} is the maximum rate observed in each data series. k_{max} (min^{-1}) values are listed above the graph (the number in parenthesis is the pH where the k_{max} value was observed for each deoxyribozyme). The pH profiles were determined at the following optimal metal ion conditions for each catalytic DNA: 500 mM Na^+ for pH3DZ1; 400 mM Na^+, 10 mM Cd^{2+} for pH4DZ1; 250 mM Na^+, 25 mM Mn^{2+} for pH5DZ1; 800 mM Na^+, 8 mM Mn^{2+}, 2 mM Ni^{2+} for pH6DZ1; 100 mM K^+, 14 mM Mn^{2+} for pH7DZ1.

CONCLUDING REMARKS

We have shown that the dual-structure forming capability possessed by all DNA aptamers can be exploited as a simple and general strategy for the engineering of fluorescence-signaling reporters that can detect the presence of aptamer targets by a coupled structure-switching/fluorescence-dequenching mechanism. The designed signaling aptamers display attractive signaling properties, including fluorescence intensity increase upon target binding, large signaling magnitude, and high target-reporting specificity. Our rational design strategy is very flexible and has the potential of being applied to any aptamer regardless of its size as well as secondary and tertiary structure properties.

It is well documented that aptamers can be readily derived from random-sequence DNA or RNA libraries by in vitro selection for binding a diverse range of targets, including proteins and metabolites. Therefore, aptamers are regarded as useful molecular tools in the burgeoning fields of proteomics and metabolomics. The simplicity and potential generality of the structure-switching design strategy, and the effectiveness of resultant fluorescence-signaling reporters, could significantly facilitate the exploration of DNA aptamers as reporter molecules for proteomic and metabolomic applications. Our next

goal is to combine in vitro selection technique and structure-switching-based rational design approach to engineer new structure-switching aptamers for the detection and quantitation of specific proteins of interest. Efforts are currently underway in our laboratory to develop structure-switching signaling aptamer-based multiplex assays that can be explored for real-time monitoring of concentration changes of various proteins in a biological pathway in response to an external stimulus. We are also assessing the possibility of entrapping metabolite-responsive structure-switching signaling aptamers inside sol-gel to produce surface-bound aptamer biosensors for metabolite detection. The progress from these studies will be reported in the future.

We have also shown that efficient, RNA-cleavage-based, fluorescence-signaling DNA enzymes can be created de novo by in vitro selection under normal or even demanding reaction conditions. The derived catalytic DNA reporters possess a uniquely synchronized chemical catalysis/real-time signaling capability because they perform an RNA-cleaving reaction toward a chimeric RNA/DNA substrate at the lone RNA linkage surrounded by a closely spaced fluorophore-quencher pair. The extremely short distance between *F* and *Q* gives rise to the maximal fluorescence quenching in the uncleaved substrate and produces a very large fluorescence enhancement upon the breakage of the RNA linkage. The covalent attachment of *F* and *Q* onto the substrate prohibits undesirable long-range movement of the fluorophore and the quencher away from each other so that the potential for false signaling that does not originate from chemical catalysis can be minimized. Another advantage of such a system is that both the catalytic and signaling components are present in a single molecule, thus, the potential exists for the development of "reagentless" sensors based on immobilization of the DNAzyme onto a suitable surface.

Our next goal is to isolate more and better signaling DNA enzymes that carry different fluorophores and quenchers and use these DNA enzymes and various high-affinity and high-specificity DNA aptamers to construct multiplexed, real-time signaling, allosteric deoxyribozyme reporters. The aptamer domains of the envisioned allosteric DNA enzymes will act as target detectors, and the catalytic domains will function as signal generators and amplifiers. Such catalytic DNA systems are deemed highly desirable in the fields of proteomics and metabolomics and should have the capability to report several proteins or metabolites simultaneously at low concentrations and in real time.

ACKNOWLEDGMENTS

We thank members of the Li laboratory for helpful discussions. This work was supported by research grants from the Canadian Institutes of Health Research, the Natural Sciences and Engineering Research Council of Canada, and Canadian Foundation for Innovation. Y.L. is a Canada Research Chair.

REFERENCES

1. K. Kruger, P. J. Grabowski, A. J. Zaug, J. Sands, D. E. Gottschling, T. R. Cech. *Cell* **31**, 147–157 (1982).
2. C. Guerrier-Takada, K. Gardiner, T. Marsh, N. Pace, S. Altman. *Cell* **35**, 849–857 (1983).
3. D. P. Bartel and J. W. Szostak. *Science* **261**, 1411–1418 (1993).
4. R. R. Breaker and G. F. Joyce. *Chem. Biol.* **1**, 223–229 (1994).
5. C. Tuerk and L. Gold. *Science* **249**, 505–510 (1990).
6. A. D. Ellington and J. W. Szostak. *Nature* **346**, 818–822 (1990).
7. M. Famulok, G. Mayer, M. Blind. *Acc. Chem. Res.* **33**, 591–599 (2000).
8. D. S. Wilson and J. W. Szostak. *Annu. Rev. Biochem.* **68**, 611–647 (1999).
9. D. Sen and C. R. Geyer. *Curr. Opin. Chem. Biol*. **2**, 680–687 (1998).
10. Y. Li and R. R. Breaker. *Curr. Opin. Struct. Biol.* **9**, 315–323 (1999).
11. A. Jaschke. *Curr. Opin. Struct. Biol.* **11**, 321–326 (2001).
12. G. M. Emilsson and R. R. Breaker. *Cell Mol. Life Sci.* **59**, 596–607 (2002).

13. N. Carmi, L. Shultz, R. R. Breaker. *Chem. Biol.* **3**, 1039–1046 (1996).
14. S. W. Santoro and G. F. Joyce. *Proc. Nat. Acad. Sci. USA* **94**, 4262–4266 (1997).
15. Y. Wang and S. K. Silverman. *J. Am. Chem. Soc.* **125**, 6880–6881 (2003).
16. Y. Li and R. R. Breaker. *Proc. Natl. Acad. Sci.* **96**, 2746–2751 (1999).
17. R. P. Fahlman and D. Sen. *J. Am. Chem. Soc.* **124**, 4610–4616 (2002).
18. J. Fritz, M. K. Baller, H. P. Lang, H. Rothuizen, P. Vettiger, E. Meyer, H. Guntherodt, C. Gerber, J. K. Gimzewski. *Science* **288**, 316–318 (2000).
19. M. Liss, B. Petersen, H. Wolf, E. Prohaska. *Anal. Chem.* **74**, 4488–4495 (2002).
20. R. A. Potyrailo, R. C. Conrad, A. D. Ellington, G. M. Hieftje. *Anal. Chem.* **70**, 3419–3425 (1998).
21. J. R. Lakowicz. *Principles of Fluorescence Spectroscopy*, 2nd ed., Kluwer Academic/Plenum, New York (1999).
22. S. Jhaveri, R. Kirby, R. Conrad, E. Maglott, M. Bowser, R. T. Kennedy, G. Glick, A. D. Ellington. *J. Am. Chem. Soc.* **122**, 2469–2473 (2000).
23. S. Jhaveri, M. Rajendran, A. D. Ellington. *Nat. Biotechnol.* **18**, 1293–1297 (2000).
24. N. Hamaguchi, A. Ellington, M. Stanton. *Anal. Biochem.* **294**, 126–131 (2001).
25. R. Yamamoto, T. Baba, P. K. Kumar. *Genes Cells* **5**, 389–396 (2000).
26. M. N. Stojanovic, P. de Prada, D. W. Landry. *J. Am. Chem. Soc.* **122**, 11547–11548 (2000).
27. M. N. Stojanovic, P. de Prada, D. W. Landry. *J. Am. Chem. Soc.* **123**, 4928–4931 (2001).
28. J. J. Li, X. Fang, W. Tan. *Biochem. Biophys. Res. Commun.* **292**, 31–40 (2002).
29. R. Nutiu and Y. Li. *J. Am. Chem. Soc.* **125**, 4771–4778 (2003).
30. J. Li and Y. Liu. *J. Am. Chem. Soc.* **122,** 10466–10467 (2000).
31. M. N. Stojanovic, P. de Prada, D. W. Landry. *Nucleic Acids Res.* **28**, 2915–2918 (2000).
32. M. N. Stojanovic, P. de Prada, D. W. Landry. *Chembiochem.* **2**, 411–415 (2001).
33. A.V. Todd, C. J. Fuery, H. L. Impey, T. L. Applegate, M. A. Haughton. *Clin. Chem.* **46**, 625–630 (2000).
34. S. H. J. Mei, Z. Liu, J. D. Brennan, Y. Li. *J. Am. Chem. Soc.* **125**, 412–420 (2003).
35. Z. Liu, S. H. J. Mei, J. D. Brennan, Y. Li. *J. Am. Chem. Soc.* **125**, 7539–7545 (2003).
36. D. E. Huizenga and J. W. Szostak. *Biochemistry* **34**, 656–665 (1995).
37. C. H. Lin and D. J. Patel. *Chem. Biol.* **4**, 817–832 (1997).
38. L. C. Bock, L. C. Griffin, J. A. Latham, E. H. Vermass, J. J. Toole. *Nature* **355**, 564–566 (1992).
39. K. Padmanabhan, K. P. Padmanabhan, J. D. Ferrara, J. E. Sadler, A. Tulinsky. *J. Biol. Chem.* **268**, 17651–17654 (1993).
40. M. Zuker. *Nucleic Acids Res.* **31**, 3406–3415 (2003).
41. R. R. Breaker. *Curr. Opin. Biotechnol.* **13**, 31–39 (2002).
42. S. K. Silverman. *RNA* **9**, 377–383 (2003).
43. G. A. Soukup and R. R. Breaker. *Proc. Natl. Acad. Sci. USA* **96**, 3584–3589 (1999).
44. M. P. Robertson and A. D. Ellington. *Nat. Biotechnol.* **17**, 62–66 (1999).
45. M. Koizumi, G. A. Soukup, J. N. Kerr, R. R. Breaker. *Nat. Struct Biol.* **6**, 1062–1071 (1999).
46. S. Seetharaman, M. Zivarts, N. Sudarsan, R. R. Breaker. *Nat. Biotechnol.* **19**, 336–341 (2001).
47. M. P. Robertson and A. D. Ellington. *Nat. Biotechnol.* **19**, 650–655 (2001).
48. J. S. Hartig, S. H. Najafi-Shoushtari, I. Grune, A. Yan, A. D. Ellington, M. Famulok. *Nat. Biotechnol.* **20**, 717–722 (2002).
49. M. Levy and A. D. Ellington. *Chem. Biol.* **9**, 417–426 (2002).
50. N. K. Vaish, F. Dong, L. Andrews, R. E. Schweppe, N. G. Ahn, L. Blatt, S. D. Seiwert. *Nat. Biotechnol.* **20**, 810–815 (2002).